LBL--32405

DE92 017017

# ELECTRONIC STRUCTURE OF HIGHLY CORRELATED STRUCTURES*

L. M. Falicov and J. K. Freericks

Department of Physics
University of California
Berkeley, CA 94720

and

Materials Sciences Division
Lawrence Berkeley Laboratory
Berkeley, CA 94720

May 1992

---

*This work was supported in part by the Director, Office of Energy Research, Office of Basic Energy Sciences, Materials Sciences Division of the U. S. Department of Energy under Contract No. DE-AC03-76SF00098.

# ELECTRONIC STRUCTURE OF HIGHLY CORRELATED SYSTEMS

L. M. Falicov and J. K. Freericks[*]

Department of Physics, University of California at Berkeley,
and Materials Sciences Division, Lawrence Berkeley Laboratory,
Berkeley, California, 94720, USA

## ABSTRACT

Three different but related problems are discussed in this contribution, all related to the so-called Anderson, Hubbard , and $t-J$ Hamiltonians — the prototype Hamiltonians for systems with highly correlated electrons: (1) The relationship — based on the well known canonical (Schrieffer-Wolff) transformation — between the Anderson model (in the small-hybridization and large-Coulomb-interaction regime) and the local moment, the Kondo, the Hubbard and the $t-J$ models, in particular the phenomena of rare-earth magnetism, intermediate valence, and heavy fermions; (2) The exact solution of these Hamiltonians in the periodic small-cluster approximation and the conditions for the existence of the heavy-fermion phenomenon; (3) The metamagnetic transition in heavy-fermion systems.

## 1. INTRODUCTION

Crystalline compounds that involve lanthanide or actinide ions display a rich variety of physical phenomena: long-range-ordered local magnetic moments [1] (ferromagnets, antiferromagnets, spiral or canted spin arrangements, *etc.*); the Kondo effect (a strong interaction between conduction electrons and local moments that manifests itself in an anomalous resistivity [2] and the quenching of magnetic moments everywhere [3,4]); heavy fermions [5,6] (materials characterized by a huge "density of states at the Fermi level"); intermediate valence [7] (strong charge fluctuations that produce, on average, only a fraction of an electron per ion); and band theory [8] (electrons that are approximated well by noninteracting particles).

Lanthanide and actinide compounds possess ions with localized (atomic) $f$-orbitals that do not overlap with the corresponding $f$-orbitals on neighboring ions, but do hybridize with the extended states of the conduction-band electrons. The $f$-electrons interact very strongly with each other via a screened (on-site) Coulomb interaction $U$ that acts only between two $f$-electrons that are localized about the same lattice site. The Coulomb energy is larger than any other in the problem ($U > 10$ eV) so that at each site only two possible occupations of the $f$-shell exist: $(4f)^n$, and $(4f)^{n+1}$. For the sake of definiteness and simplicity a single $f$ orbital site is considered here ($n$ is taken to be 0); doubly occupied $f$-orbitals, because of the large $U$, are effectively forbidden. The physics of such an electronic system is described by the lattice (or periodic) Anderson impurity model [9]

$$H_A = \sum_{k\sigma} \varepsilon_k a_{k\sigma}^{\dagger} a_{k\sigma} + \varepsilon \sum_{i\sigma} f_{i\sigma}^{\dagger} f_{i\sigma} + U \sum_{i} f_{i\uparrow}^{\dagger} f_{i\uparrow} f_{i\downarrow}^{\dagger} f_{i\downarrow} + \sum_{ik\sigma} [V_{ik} f_{i\sigma}^{\dagger} a_{k\sigma} + V_{ik}^{*} a_{k\sigma}^{\dagger} f_{i\sigma}] \quad , \tag{1}$$

in the large-$U$ limit. (This limit, as understood here, implies both $U \to \infty$ and $\varepsilon + U \to \infty$, so that there is never more than one electron per $f$-orbital.) The parameters and operators in Eq. (1) include the conduction-band creation (annihilation) operators $a_{k\sigma}^{\dagger}$ ($a_{k\sigma}$) for a conduction electron in an extended state with wavevector $k$, spin $\sigma$, and energy $\varepsilon_k$; the

localized electron creation (annihilation) operators $f_{i\sigma}^{\dagger}$ ($f_{i\sigma}$) for localized electrons in an atomic orbital centered at lattice site $i$ with energy $\varepsilon$; the on-site Coulomb interaction $U$; and the hybridization integral $V_{ik}$ that mixes together the localized and extended states. (As already mentioned, the degeneracy of the $f$-electrons is neglected here; additional $f$-electron orbitals may easily be added without changing the qualitative nature of the model.) The hybridization integral $V_{ik}$ is assumed to be of the form

$$V_{ik} = \exp(i\,\mathbf{R}_i \cdot \mathbf{k})\, V\, g(k)/\sqrt{N} \quad , \tag{2}$$

with $g(k)$, the form factor, a dimensionless function of order one, and $N$ the number of lattice sites. The Fermi level $E_F$ is defined to be the maximum energy of the filled conduction band states, in the limit $V \to 0$, and the origin of the energy scale is chosen so that $E_F = 0$. The conduction-band density of states per site at the Fermi level is then defined to be $\rho$.

## 2. THE SCHRIEFFER-WOLFF TRANSFORMATION OF THE LATTICE ANDERSON IMPURITY MODEL: LOCAL MOMENTS, KONDO LATTICE, HEAVY FERMIONS, INTERMEDIATE VALENCE, AND BAND THEORY

The lattice Anderson impurity model can be exactly diagonalized in two limits: in the noninteracting case ($U\rho \to 0$) the Hamiltonian is a quadratic form in the fermionic operators, *i.e.* an independent particle problem, and can be diagonalized by a change in one-particle basis; in the zero hybridization limit ($V\rho \to 0$) the Hamiltonian decouples into two independent systems (extended electrons and localized electrons), with explicitly diagonal sub-Hamiltonians for each subsystem. The large-interaction ($U\rho \gg 1$), small-hybridization ($V\rho \ll 1$) limit of the Anderson model is the physically relevant regime for studying lanthanide and actinide compounds. Exact diagonalization studies [10] (on small systems) show that the lattice Anderson impurity model can describe all of the physical phenomena (local moments, Kondo effect, heavy fermions, intermediate valence, and band theory) of lanthanide and actinide compounds simply by varying the parameter $\varepsilon\rho$ from large negative values to large positive values. In fact, the lattice Anderson impurity model, in the infinite-$U$ and $V\rho \ll 1$ limit, is characterized by five regimes depending upon the localized-electron energy $\varepsilon$ (see Figure 1):

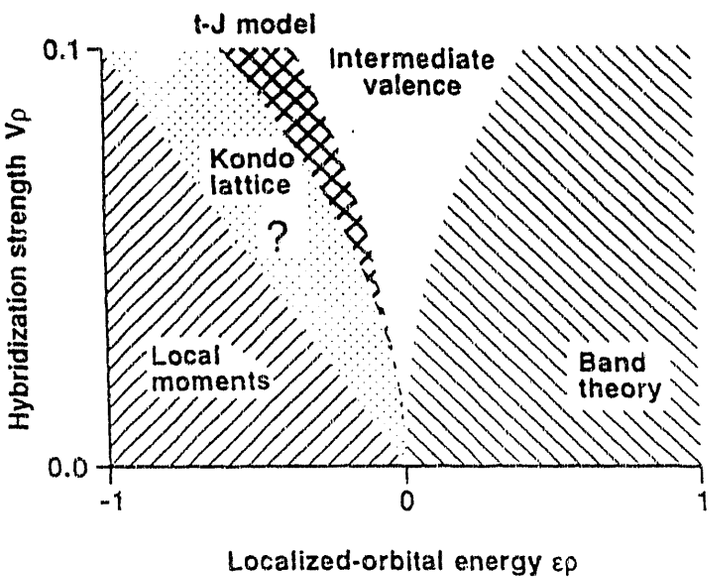


Figure 1. A schematic diagram showing the regions of parameter space where local magnetic moments, Kondo lattice [11,12] (quenched moments everywhere), $t$–$J$ model, intermediate valence, and one-electron band theory are expected to occur in the small hybridization, large interaction strength limit of the lattice Anderson impurity model. The horizontal axis records the localized $f$-electron energy (relative to the Fermi level) and the vertical axis records the hybridization strength. Heavy-fermion behavior may occur in the transition region between the Kondo lattice and intermediate valence ($t$–$J$ model regime). A fine-tuning of the parameters and the crystal structure of the (effective) $t$–$J$ model is required to produce a heavy-fermion system.

(A) $\epsilon\rho \ll -V\rho < 0$ — isolated local moments [1,8]. In this limit the $f$-orbitals are occupied by a single electron ($<f_{i\uparrow}^{\dagger} f_{i\uparrow} + f_{i\downarrow}^{\dagger} f_{i\downarrow} > = 1$), and (effectively) decoupled from the conduction electrons. There are everywhere local magnetic moments. The local moments interact with each other via exchange, superexchange, and/or Ruderman-Kittel-Kasuya-Yosida (RKKY) interactions [1] with ferromagnetic or antiferromagnetic exchange integrals. The rich magnetic structure of the rare-earth metals appears in this regime.

(B) $-V\rho \ll \epsilon\rho \ll -V^2\rho^2 < 0$ — the regime where the Kondo effects holds for impurities and where a Kondo lattice [11,12] may exist. In this regime there are no charge excitations in the localized orbitals ($<f_{i\uparrow}^{\dagger} f_{i\uparrow} + f_{i\downarrow}^{\dagger} f_{i\downarrow} > = 1$), but the local moments interact strongly with conduction-electron spins at the Fermi level to quench the magnetic moments everywhere.

(C) $\epsilon\rho \approx -V^2\rho^2$ — the $t$-$J$ model [6]. In this regime the localized orbitals are almost singly occupied ($<f_{i\uparrow}^{\dagger} f_{i\uparrow} + f_{i\downarrow}^{\dagger} f_{i\downarrow} > = 1-\nu$ , $\nu \ll 1$) and have broadened into a strongly correlated narrow band in which all electronic transport takes place; the conduction band is (effectively) decoupled and acts only as a buffer that determines the concentration of electrons in the narrow band.

(D) $-V^2\rho^2 \ll \epsilon\rho \ll V^2\rho^2$ — intermediate valence [7]. As $\epsilon$ is increased to the Fermi level and beyond the occupation of the localized orbitals becomes nonintegral ($0 < <f_{i\uparrow}^{\dagger} f_{i\uparrow} + f_{i\downarrow}^{\dagger} f_{i\downarrow} > < 1$) and the system is in the intermediate valence regime.

(E) $0 < V^2\rho^2 \ll \epsilon\rho$ — band theory [8]. As $\epsilon$ is increased well beyond the Fermi level all localized states are essentially unoccupied ($<f_{i\uparrow}^{\dagger} f_{i\uparrow} + f_{i\downarrow}^{\dagger} f_{i\downarrow} > \approx 0$) and (effectively) decoupled from the conduction electrons. The ground state is determined by one-electron band theory for the extended electronic states, which exhibit a very small hybridization with the $f$-states.

Heavy-fermionic behavior [5,6] occurs, *under certain circumstances*, in regime (C), the transition region from the Kondo-lattice [11] regime (B) to the intermediate-valence regime (D). The many-body ground state is characterized by a huge number of low-lying excited states that have many different spin configurations (a partial decoupling of spatial and spin degrees of freedom) and is close to a disproportionation instability. This produces a very large coefficient to the term linear in temperature in the specific heat, a large magnetic susceptibility, and poor metallic conductivity.

The five regimes outlined above may be established by employing a Schrieffer-Wolff [13] canonical transformation to the lattice Anderson impurity model. Since the details of this transformation are well known [13,14], only an outline will be presented here.

The Anderson Hamiltonian $H_A$ is divided into two terms $H_A = H_0 + H_{hyb}$ where $H_{hyb}$ is the last term in Eq. (1). A canonical transformation $H' = \exp(S) H_A \exp(-S)$ is performed with $S$ chosen to satisfy $[H_0, S] = H_{hyb}$. One finds (to lowest order in $V$) that $H' = H_0 + \frac{1}{2}[S, H_{hyb}]$ or

$$H' - H_0 = -\sum_{ikk'} J_{ikk'} \, \psi_{fi}^{\dagger} \boldsymbol{\sigma} \psi_{fi} \cdot \psi_k^{\dagger} \boldsymbol{\sigma} \psi_{k'} \tag{3a}$$

$$- \sum_{ii'k\sigma} [W_{ii'kk} + \frac{1}{4} J_{ii'kk} \, (f_{i-\sigma}^{\dagger} f_{i-\sigma} + f_{i'-\sigma}^{\dagger} f_{i'-\sigma})] f_{i\sigma}^{\dagger} f_{i'\sigma} \tag{3b}$$

$$+ \sum_{ikk'} [W_{iikk'} + \frac{1}{4} J_{iikk'} \, \psi_{fi}^{\dagger} \psi_{fi}] \, \psi_k^{\dagger} \psi_{k'} \tag{3c}$$

$$+ \frac{1}{4} \sum_{ikk'\sigma} [K_{iikk'} \, f_{i\sigma}^{\dagger} f_{i-\sigma}^{\dagger} \, a_{k\sigma} a_{k'-\sigma} + h.c.] \quad , \tag{3d}$$

where the spinors are defined to be

$$\psi_k \equiv \begin{bmatrix} a_{k\uparrow} \\ a_{k\downarrow} \end{bmatrix} \quad , \qquad \psi_{fi} \equiv \begin{bmatrix} f_{i\uparrow} \\ f_{i\downarrow} \end{bmatrix} \quad , \tag{4}$$

$\boldsymbol{\sigma}$ denotes the Pauli spin matrices, and the coefficients are

$$J_{ii'kk'} \equiv V_{ik} V_{i'k'}^{*} \left[ \frac{1}{\epsilon_k - \epsilon - U} + \frac{1}{\epsilon_{k'} - \epsilon - U} - \frac{1}{\epsilon_k - \epsilon} - \frac{1}{\epsilon_{k'} - \epsilon} \right] \quad , \tag{5a}$$

$$K_{ii'kk'} \equiv V_{ik} V_{i'k'} \left[ \frac{1}{\epsilon_k - \epsilon - U} + \frac{1}{\epsilon_{k'} - \epsilon - U} - \frac{1}{\epsilon_k - \epsilon} - \frac{1}{\epsilon_{k'} - \epsilon} \right] \quad , \tag{5b}$$

$$W_{ii'kk'} \equiv \tfrac{1}{2} V_{ik} V^{*}_{i'k'} \left[ \frac{1}{\varepsilon_k - \varepsilon} + \frac{1}{\varepsilon_{k'} - \varepsilon} \right] \quad . \tag{5c}$$

The last term (3d) can always be neglected (in the large-$U$ limit) because it only connects configurations that have zero electrons at site $i$ to configurations with two electrons at site $i$, which are explicitly forbidden.

The canonical transformation of the lattice Anderson impurity model is approximated well by the lowest order term (in $V$) when $|V^2\rho/\varepsilon| < 1$. In this region of parameter space the localized orbitals have an occupancy per site close to one ($\varepsilon < 0$) or close to zero ($\varepsilon > 0$). When the occupancy is close to one, the operator $\psi^{\dagger}_{fi}\psi_{fi}$ may be replaced by unity and both the term (3c) and the diagonal ($i = i'$) terms in (3b) may be absorbed into a renormalized $H_0$. The remaining terms in Eq. (3) describe spin scattering of the conduction electrons at the Fermi level by the localized moments (3a), and direct hopping terms within the (narrow) $f$-band (3b). When the occupancy is close to zero — the band-theory regime — the operators $\psi^{\dagger}_{fi}\psi_{fi}$, $\psi^{\dagger}_{fi}\sigma\psi_{fi}$, and $f_i^{\dagger}f_{i'}$ may all be replaced by zero. The only important terms remaining in Eq. (3) are the changes in the one-particle band-structure arising from (3c).

The local-moment regime corresponds to the case where $\varepsilon\rho \ll -V\rho < 0$ so that $|J_{ii'kk'}| \ll 1$ for $k$ and $k'$ at the Fermi surface. To lowest order, the ground state consists of one $f$-electron per site and a conduction band filled up to energy $E_F$. The spin flipping of the local moments by the conduction-band electrons at the Fermi surface (3a) is weak and all other terms in Eq. (3) can be neglected. The interaction (3a) between localized spins and conduction electrons then leads, through $H_0$, to a variety of localized-spin exchange interactions [15]. These, in turn, determine, at low enough temperatures, the long-range magnetic order.

The Kondo-lattice model [11,12] corresponds to the case where $-V\rho \ll \varepsilon\rho \ll -V^2\rho^2 < 0$, the $f$-orbitals are singly occupied (so that the hopping term (3b) may be neglected), and the density of states of the conduction electrons is not negligible at the Fermi level, so that the spin scattering term (3a) is the most important correction term. The local-moment spins strongly interact with the conduction electrons (at the Fermi surface) which quench the magnetic moments everywhere.

The $t$–$J$ model occurs in the region where $\varepsilon\rho \approx -V^2\rho^2 < 0$. The localized states broaden into a narrow band with an occupancy of *nearly* one electron per site; the density of states of the conduction electrons at the Fermi level is negligible, so that the spin-scattering term (3a) may be neglected. In this case, the hopping term (3b) is the most important correction term. The conduction electrons are decoupled from the $f$-band and act only as a buffer that determines the filling of the $f$-band. The hole density $v$ required for the hopping term (3b) to be more important than the spin-scattering term (3a) is

$$\left| \frac{\sum_{FS} g^2(k)/\varepsilon}{\sum_{BZ} g^2(k) \exp(i\,\mathbf{k}\cdot\boldsymbol{\tau})/(\varepsilon_k - \varepsilon)} \right| \ll v \ll 1 \quad , \tag{6}$$

where $\tau$ is a nearest-neighbor translation vector, FS denotes a summation over wavevectors that lie on the Fermi surface only, and BZ denotes a summation over all wavevectors in the Brillouin zone.

This narrow $f$-band is described by the large-$U$ limit of the Hubbard model [16], which in turn becomes the $t$–$J$ model [17]

$$H_{t\text{-}J} = -\sum_{ij\sigma} t_{ij} (1 - f_{i-\sigma}^{\dagger} f_{i-\sigma}) f_{i\sigma}^{\dagger} f_{j\sigma} (1 - f_{j-\sigma}^{\dagger} f_{j-\sigma}) + \sum_{ij} J_{ij}\, \mathbf{S}_i \cdot \mathbf{S}_j \quad , \tag{7}$$

with

$$t_{ij} = \sum_k W_{ijkk} = \sum_k \frac{V^{*}_{ik} V_{jk}}{\varepsilon_k - \varepsilon} \quad , \tag{8}$$

and $J_{ij} = 4|t_{ij}|^2/U$. Note that the hopping matrix elements $t_{ij}$ in Eq. (8) are short-ranged, *i.e.*, strongly peaked functions of the separation $|\mathbf{R}_i - \mathbf{R}_j|$ between lattice sites $i$ and $j$, as expected.

A *necessary* condition for heavy-fermion behavior is that the parameters of the Anderson model fall into the range where the mapping onto the $t$–$J$ model is valid, but this condition is *not sufficient*. The solutions of the $t$–$J$ model must also possess a very large number of low-lying excitations with many different spin configurations. This latter

condition requires a *fine-tuning* of the parameters in the $t$–$J$ model and depends strongly upon the geometry and connectivity of the lattice. For example, exact-diagonalization calculations on small clusters [18,19] — see below — indicate that strongly frustrated lattices, for occupancy close to one electron per site, are the best candidates for heavy-fermionic behavior (*e.g.*, the system with 7 electrons in an eight-site face-centered-cubic cluster possesses solutions with strongly enhanced low-temperature specific heat, quasielastic spin excitations, and poor metallic conductivity; the ground state may be magnetic or nonmagnetic).

The intermediate-valence regime occurs when the Schrieffer-Wolff transformation may not be truncated to lowest order, $|\varepsilon\rho| \ll V^2\rho^2$, or its expansion may not be valid at all. In this case, all parameters are equally important and the full many-body problem must be solved. The average occupation (per site) of an $f$-orbital decreases from 1 to 0 as $\varepsilon\rho$ is increased. This regime has been studied by mapping onto a Fermi liquid [7] and by exact-diagonalization on small clusters [10].

Finally in the region where $\varepsilon\rho \gg V^2\rho^2$, the Schrieffer-Wolff transformation is once again valid to lowest order and one finds that the $f$-orbitals are completely empty and (effectively) decoupled from the conduction band. The system is described by one-electron theory [8] for the conduction-band electrons alone. This is the regime where ordinary density-functional theory is an excellent tool for calculating the electronic properties.

## 3. PERIODIC SMALL-CLUSTER APPROACH TO MANY-BODY PROBLEMS IN GENERAL, AND HEAVY-FERMION SYSTEMS IN PARTICULAR

It is known from the basic duality between real and reciprocal spaces [8] that a microcrystal of $N$ sites with periodic boundary conditions has eigenstates that can be classified by $N$ $k$-vectors, distributed periodically throughout the Brillouin zone. Conversely, the sampling of $N$ points, periodically distributed in the Brillouin zone is equivalent to solving a problem in real space, in a microcrystal of $N$ sites with periodic boundary conditions. This method has been extensively used by the authors, their collaborators, and others [10, 18-21] to solve a variety of problems, both model Hamiltonians and realistic situations [22-24].

The cluster is chosen to be small enough that the many-body Hamiltonian may be exactly diagonalized but (hopefully) large enough that the physics of the infinite lattice is captured. For the heavy-fermion case discussed below, the mapping of the Anderson model (1) onto a $t$–$J$ model reduces the size of the Hilbert space by a factor of $(3/16)^N$ which allows larger clusters to be studied.

An understanding of exactly how to extrapolate the results for a small-cluster calculation to the thermodynamic limit ($N \rightarrow \infty$) has not yet been achieved. It is nonetheless obvious that some very interesting effects are observed in these small clusters (small $k$-space sampling), and one such effect is the appearance of heavy-fermion behavior.

### 3(a). A Heavy-Fermion Case in a Small-Cluster t-J Model

The small-cluster approach has been applied to the $t$–$J$ model [18-19]. A very good example of a heavy-fermion system lies in an eight-site face-centered cubic-lattice cluster with seven electrons [18-19]. When the hopping parameters and antiferromagnetic superexchange parameters are chosen to be

$$t_{ij} = \begin{cases} t > 0\,, & i\,,j \ = \text{first–nearest neighbors}\,, \\ t' = 0.1t\,, & i\,,j \ = \text{second–nearest neighbors}\,, \\ 0\,, & \text{otherwise}\,, \end{cases}$$

$$J_{ij} = \begin{cases} J\,, & i\,,j \ = \text{first–nearest neighbors}\,, \\ 0\,, & \text{otherwise}\,, \end{cases} \tag{9}$$

(out of a total of 1024 states) that is split-off from the higher-energy excitations and which include many different spin configurations (see Table 1). These many-body states are degenerate at $J=0$ but the degeneracy is partially lifted for finite $J$, with low-spin configurations favored (energetically) over high-spin configurations. It is worth remarking that even with the antiferromagnetic interaction included, the spin 1/2 ground state remains accidentally degenerate, with a degeneracy of 14, *i.e.*, 14% of the available states remain in the ground-state manifold.

| Energy | Total Spin | Degeneracy | Spatial Symmetry Label |
|---|---|---|---|
| $-6t+6t'-3J$ | ½ | 14 | $\Gamma_2 \oplus X_1 \oplus X_2$ |
| $-6t+6t'-2J$ | ½ | 16 | $L_3$ |
| $-6t+6t'-1.5J$ | 1 ½ | 32 | $\Gamma_{12} \oplus X_1 \oplus X_2$ |
| $-6t+6t'-0.5J$ | 1 ½ | 16 | $L_2$ |
| $-6t+6t'+J$ | 2 ½ | 18 | $X_2$ |

Table 1. Low-energy manifold of many-body eigenstates, at zero magnetic field, for the model heavy-fermion system discussed in the text. The notation is that of References [18,19].

## 4. HEAVY-FERMIONS IN MAGNETIC FIELDS: THE METAMAGNETIC TRANSITION

Heavy-fermion systems have been an active area of research for both experimentalists [5] and theorists [6] since their discovery in the mid-1970's. Heavy-fermion systems are characterized by huge coefficients ($\gamma$) to the term linear in $T$ in the specific heat, quasi-elastic spin excitations (large magnetic susceptibility), and poor metallic conductivity. These features may be qualitatively described by a Fermi liquid with a very large density of states at the Fermi level [6]. Heavy-fermion systems may become superconductors ($UPt_3$, $UBe_{13}$, $CeCu_2Si_2$, $URu_2Si_2$, *etc.*), possess long-range magnetic order ($UPt_3$, $URu_2Si_2$, $NpBe_{13}$, $U_2Zn_{17}$, *etc.*), or remain paramagnetic metals ($CeRu_2Si_2$, $CeAl_3$, $CeCu_6$, *etc.*) at low temperatures.

Recent experimental work has concentrated on the properties of heavy-fermion systems in high magnetic fields [25-28]. A "transition" is observed (the so-called metamagnetic transition) at a characteristic magnetic field $B_c$ in $CeRu_2Si_2$ ($B_c = 7.8T$), $UPt_3$ ($B_c = 21T$), and $URu_2Si_2$ ($B_c = 36T$). The transition is characterized by a magnetic-field dependence of the coefficient $\gamma$, the elastic coefficients, and the magnetic properties. At the critical field $B_c$, the coefficient $\gamma$ has a single peak, the elastic coefficients are softened, and the magnetic fluctuations change character. The magnetization shows a steplike structure as a function of magnetic field strength. This contribution presents a many-body theory (*without* the assumptions of Fermi-liquid theory) that describes all of the above electronic properties of heavy-fermion systems (except superconductivity) and their field dependence.

Every heavy-fermion system is composed of ions with localized $f$-orbitals (lanthanides and actinides) that do not overlap with the corresponding $f$-orbitals on neighboring ions, but do hybridize with the extended states of the conduction-band electrons. The $f$-electrons interact very strongly with each other via a screened (on-site) Coulomb interaction $U$ that acts only between two $f$-electrons that are localized about the same lattice site. Doubly occupied $f$-orbitals are effectively forbidden, since the Coulomb energy is larger than any other energy in the problem ($U > 10$ eV). The physics of such an electronic system is therefore described by the periodic Anderson impurity model [9] in the large-$U$ ($U \rightarrow \infty$) limit, Eq. (1).

Heavy-fermionic behavior may occur in the restricted region [13,14] of parameter space where $-V\rho \ll \varepsilon\rho \ll -V^2\rho^2 < 0$. The localized orbitals are *almost* singly occupied ($< f_{i\uparrow}^{\dagger} f_{i\uparrow} + f_{i\downarrow}^{\dagger} f_{i\downarrow} > = 1-\nu$ ; $\nu \ll 1$) and the conduction electron density of states at the Fermi level is small. In this case, the kinetic energy of the holes that hop within a narrow "effective" band dominates over the magnetic spin-spin interactions and the spin-flipping terms of the Kondo effect.

The renormalized Schrieffer-Wolff transformation of the lattice Anderson model is then well described by a $t$-$J$ model in the limit $|V^2\rho/\varepsilon| \ll 1$. When $\rho\varepsilon \ll -V\rho < 0$, the renormalized magnetic interactions $J$ between the local moments of the $f$-electrons dominate. The local moments interact with each other via all forms of exchange interactions, which determine, at low enough temperatures, the long-range magnetic order. As $\rho\varepsilon$ increases, two effects occur:

(i) the kinetic energy of the holes in the narrow $f$-band become important; and

(ii) a residual Kondo effect begins to quench the local magnetic moments.

In this regime,

$$-V\rho \ll \varepsilon\rho \ll -V^2\rho^2 \quad , \tag{8}$$

the Anderson model is approximated well by the full $t$-$J$ model. The conduction electrons

are decoupled from the $f$-band and act only as a buffer that determines the filling of the $f$-band. This picture is supported by numerical evidence found in exact solutions [19-21] of the lattice Anderson model on four-site clusters (see the next section).

### 4(a). Heavy-Fermionic Behavior in the t–J Model

A heavy-fermion system is characterized by a many-body ground state with very large number of low-lying excited states that have many different spin configurations (a partial decoupling of spatial and spin degrees of freedom). The localized states broaden into a strongly correlated narrow band in which all electronic transport takes place; the conduction band is (effectively) decoupled and acts only as a buffer that determines the concentration of electrons in the narrow band. The formation of a heavy-fermion ground state (and its low-lying excitations) require a fine-tuning of the parameters in the (effective) $t$–$J$ model and depends strongly upon the geometry and connectivity of the lattice.

### 4(b). The Metamagnetic Transition

As seen in the example of the previous section (Table I), the ground-state manifold of a heavy-fermion system contains a very large number of almost degenerate state. In that example there are 96 many-body states — out of a total of 1024 — which are degenerate for $J=0$. A finite $J$ value partially lifts that degeneracy y, with low-spin configurations energetically favored over high-spin configurations.

A magnetic field (in the $z$-direction) partially lifts the degeneracy even more, since the many-body eigenstates with $z$-component of spin $m_z$ have an energy

$$E(B) = E(0) - m_z g \mu_B B \equiv E(0) - m_z bJ \quad , \tag{10}$$

in a magnetic field $B$. The symbols $g$, $\mu_B$, and $b$ denote the Landé g-factor, Bohr magneton, and dimensionless magnetic field, respectively. The high-spin eigenstates are energetically favored in a strong magnetic field and level crossings occur as a function of $b$.

The phenomena described above are all of the necessary ingredients for a metamagnetic transition. The heavy-fermion system is described by a ground state with nearly degenerate low-lying excitations of many different spin configurations. The antiferromagnetic superexchange pushes high-spin states up in energy with splittings on the order of $J$. The magnetic field pulls down these high-spin states (with maximal $m_z$) and generates level crossings in the ground state. In the region near the level crossings, there is an increase in the density of low-lying excitations that produces a peak in the specific heat as a function of $b$. The magnetization and spin-spin correlation functions both change abruptly at the level crossings.

To illustrate the metamagnetic transition for the simple model above, the specific heat and magnetization are calculated as a function of the magnetic field (at a fixed low temperature). The specific heat satisfies

$$\frac{C_V(b)}{k_B} = \beta^2 \left[ \frac{\sum_n E_n^2 \exp(-\beta E_n)}{\sum_n \exp(-\beta E_n)} - \left\{ \frac{\sum_n E_n \exp(-\beta E_n)}{\sum_n \exp(-\beta E_n)} \right\}^2 \right] \quad , \tag{11}$$

where $k_B$ is Boltzmann's constant, $\beta$ is the inverse temperature ($\beta \equiv 1/k_B T$) and $E_n$ is the energy of the $nth$ many-body eigenstate in a magnetic field $b$ (the summations are restricted to the 96 eigenstates in Table 1). Similarly the magnetization is expressed by

$$M(b) = \frac{\sum_n m_z \exp(-\beta E_n)}{\sum_n \exp(-\beta E_n)} \quad , \tag{12}$$

where $m_z$ is the z-component of spin for the $nth$ many-body eigenstate. The results for the specific heat and magnetization are given in Figures 2 and 3, respectively, at the temperature where $\beta J = 1$. Results for the magnetization at a lower temperature, $\beta J = 5$ are given in Figure 4.

The specific heat at the higher temperature has a single broad peak as a function of magnetic field with the center of the peak moving to larger values of $b$ and the zero-field intercept becoming smaller as the temperature increases. The magnetization smoothly changes from a value of zero to a value of 5/2 as a function of magnetic field, showing little structure.

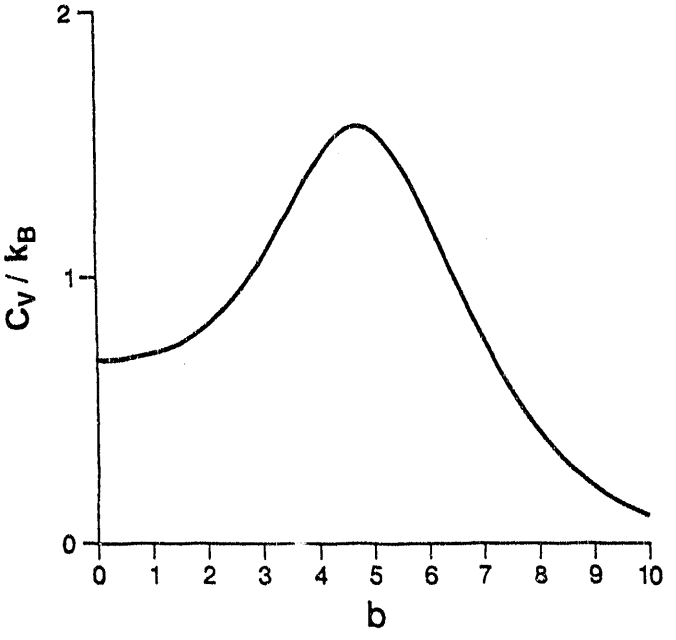


Figure 2. Calculated specific heat as a function of magnetic field for the heavy-fermion model. The temperature is $T = J/k_B$. The horizontal axis contains the dimensionless magnetic field and the vertical axis contains the dimensionless specific heat $C_V/k_B$. Note the single peak in the specific heat, characteristic of the high-temperature regime (temperature larger than the energy-level spacings).

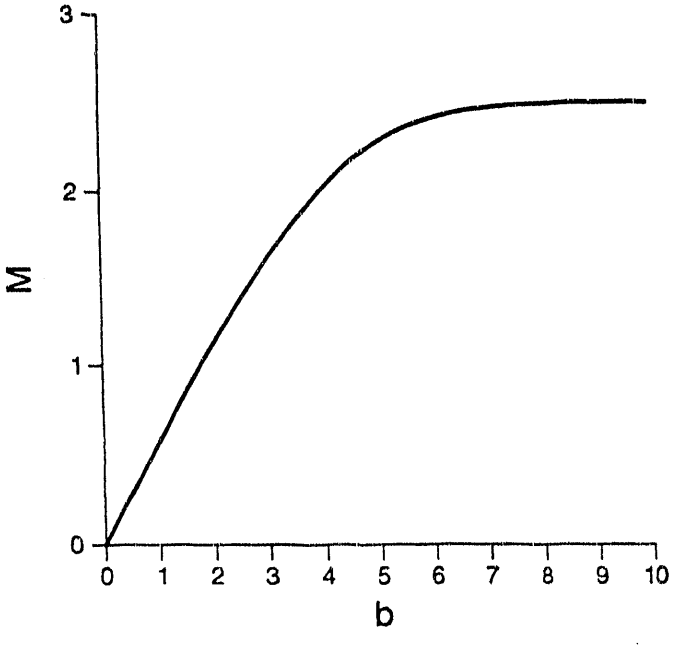


Figure 3. Calculated magnetization as a function of magnetic field at a temperature $T = J/k_B$. Note the smooth transition in the magnetization, characteristic of the high-temperature regime.

At lower temperatures the magnetization shows steps at the various values of the field where there are ground-state level crossings.

The results fit the experimental data [25-28] extremely well. The specific-heat measurements resemble the result of Figure 2 with a single-peak structure and the magnetization measurements resemble the "low-temperature" result (Figure 4) with noticeable steps. This is to be expected since magnetization measurements take place at a *constant* low temperature while specific-heat measurements require measurements over a temperature range.

Note that the low-field region ($b < 1$) is not faithfully represented by a small-cluster calculation, since the discreteness of the energy levels will always produce a linear magnetization.

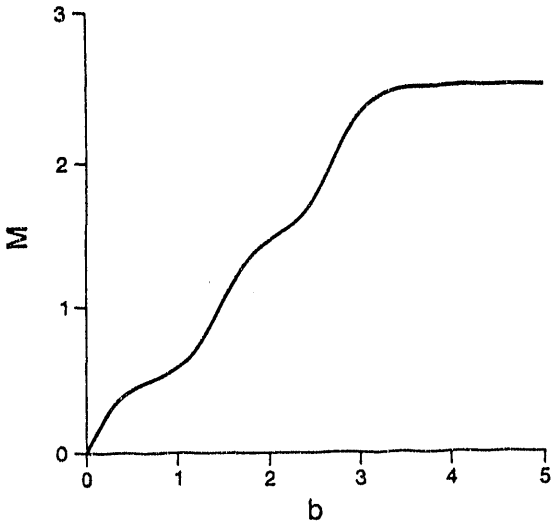


Figure 4. Calculated magnetization as a function of magnetic field at a temperature $T = J/5k_B$. Note the steplike transitions in the magnetization at each level crossing, characteristic of the low-temperature regime.

### 4(c). Discussion

The physics of the metamagnetic transition can be described as follows: a heavy-fermion system is composed of a ground-state with nearly degenerate low-lying excitations of many different spin configurations; the weak antiferromagnetic superexchange interaction slightly favors low-spin arrangements over high-spins (at zero magnetic field); a magnetic field pulls down the high-spin configurations causing (multiple) level crossing(s) in the ground state and producing a peak in the many-body density of states. The result is a peak in the specific heat (and possibly a richer structure at lower temperatures), steplike transitions in the magnetization, and abrupt changes in ground-state correlation functions.

## 5. ACKNOWLEDGMENTS

The authors acknowledge stimulating discussions with R. Fye and A. R. Mackintosh. This research was supported at the Lawrence Berkeley Laboratory, by the Director, Office of Energy Research, Office of Basic Energy Sciences, Materials Sciences Division, U.S. Department of Energy, under contract No. DE-AC03-76SF00098.

## 6. REFERENCES AND FOOTNOTES

[*] Present address: Department of Physics and Institute for Theoretical Physics, University of California, Santa Barbara, California, 93106-4030, USA

[1] J. Jensen and A. R. Mackintosh, *Rare Earth Magnetism: Structures and Excitations*, (Clarendon Press, Oxford, 1991), International Series of Monographs on Physics, Vol. 81.

[2] J. Kondo, in *Solid State Physics*, ed. F. Seitz, H. Ehrenreich and D. Turnbull, (Academic, New York, 1969), Vol. 23, p. 184.

[3] K. G. Wilson, Rev. Mod. Phys. **47**, 773 (1975) .

[4] P. B. Wiegmann im *Quantum Theory of Solids*, (Mir, Moscow, 1982), p. 238; N. Andrei, K. Furuya, and J. H. Lowenstein, Rev. Mod. Phys. **55**, 331, (1983); N. Andrei, K. Furuya, and J. H. Lowenstein, Rev. Mod. Phys. **55**, 331 (1983).

[5] G. R. Stewart, Rev. Mod. Phys. **56**, 755 (1984).

[6] C. M. Varma, Comments Sol. St. Phys. **11**, 221 (1985); P. A. Lee, T. M. Rice, J. W. Serene, L. J. Sham, and J. W. Wilkins, Comments Cond. Matt. Phys. **12**, 99, (1986); P. Fulde, J. Keller, and G. Zwicknagl, in *Solid State Physics*, ed. H. Ehrenreich and D. Turnbull, (Academic, New York, 1988), Vol. 41, p. 1.

[7] D. M. Newns and A. C. Hewson, J. Phys. F: Metal Physics **10**, 2429, (1980); *Valence Fluctuations in Solids*, ed. L. M. Falicov, W. Hanke, and M. B. Maple (North-Holland, Amsterdam, 1981); *Valence Instabilities*, ed. P. Wachter and H. Boppart (North-Holland, Amsterdam, 1982).

[8] C. Kittel, *Quantum Theory of Solids* (Wiley, New York, 1987).

[9] P. W. Anderson, Phys. Rev. **124**, 41, (1961).

[10] S. Asada and S. Sugano, J. Phys. C **11**, 3911, (1978); R. G. Arnold and K. W. H. Stevens, *ibid.* **12**, 5037 (1979); R. Jullien and R. M. Martin, Phys. Rev. B **26**, 6173, (1982); J. C. Parlebas, R. H. Victora, and L. M. Falicov, J. Physique **47**, 1029, (1986); J. C. Parlebas, R. H. Victora, and L. M. Falicov, J. Magn. Magn. Mater. **54/57**, 405, (1986); A. Reich and L. M. Falicov, Phys. Rev. B **34**, 6752, (1986); P. K. Misra, D. G. Kanhere, and J. Callaway, *ibid.* **35**, 5013, (1987); J. Callaway, D. P. Chen, D. G. Kanhere, and P. K. Misra, *ibid.* **38**, 2583 (1988); J. Callaway and D. P. Chen, J. Appl. Phys. **64**, 5944 (1988); D. P. Chen and J. Callaway, Phys. Rev. B **38**, 11869 (1988); J. C. Parlebas, Phys. Stat. Sol. (b) **160**, 11 (1990).

[11] The Kondo effect arises from a resonance of the localized electrons with the conduction electrons that quenches the localized magnetic moments. It is a non-perturbative effect which is small in magnitude and is not directly present in any model (such as the $t$–$J$ model) that projects out the conduction electron degrees of freedom. The physics of the Kondo effect in the presence of a single impurity is well known (References [2-4]). The case of a lattice of impurities is still controversial. Large-$N$ expansions show a quenching of magnetic moments everywhere (Reference [12]) but are always in the atomic limit (Reference [6]) and do not illustrate what happens in the dense "impurity" limit.

[12] S. Doniach, in *Theoretical and Experimental Aspects of Valence Fluctuations and Heavy Fermions*, edited by C. Gupta and S. K. Malik (Plenum, New York, 1987) p. 179.

[13] J. R. Schrieffer and P. A. Wolff, Phys. Rev. **149**, 491, (1966).

[14] L. C. Lopes, R. Jullien, A. K. Bhattacharjee, and B. Coqblin, Phys. Rev. B **26**, 2640 (1982); J. M. Wills and B. R. Cooper, *ibid.* **36**, 3809, (1987).

[15] C. E. T. Gonçalves da Silva and L. M. Falicov, J. Phys. C: Solid State Phys. **5**, 63, (1972).

[16] J. Hubbard, Proc. R. Soc. London, Ser. A **276**, 238 (1963); **277**, 237 (1964); **281**, 401 (1964); **285**, 542 (1965); **296**, 82, (1967); **296**, 100 (1967).

[17] A. B. Harris and R. V. Lange, Phys. Rev. **157**, 295 (1967); A. H. MacDonald, S. M. Girvin, and D. Yoshioka, Phys. Rev. B **37**, 9753 (1988); A. M. Oleś, *ibid.* **41**, 2562 (1990); A. H. MacDonald, S. M. Girvin, and D. Yoshioka, *ibid.* **41**, 2565, (1990).

[18] A. Reich and L. M. Falicov, Phys. Rev. B **37**, 5560 (1980); **38**, 11199, (1988).

[19] J. K. Freericks and L. M. Falicov, Phys. Rev. B **42**, 4960 (1990).

[20] L. M. Falicov, in *Recent Progress in Many-body Theories*, edited by A. J. Kallio, E. Pajanne, and R. F. Bishop (Plenum, New York, 1988), Vol. 1, p. 275.

[21] J. Callaway, Physica B **149**, 17 (1988).

[22] R. H. Victora and L. M. Falicov, Phys. Rev. Lett. **55**, 1140 (1985).

[23] E. C Sowa and L. M. Falicov, Phys. Rev. B **35**, 3765 (1987); *ibid.* **37**, 8707 (1988).

[24] C. Chen and L. M. Falicov, Phys. Rev. B **40**, 3560 (1989); C. Chen, Phys. Rev. Lett. **41**, 1320 (1990).

[25] C. Paulsen, A. Lacerda, L. Puech, P. Haen, P. Lejay, J. L. Tholence, and A. de Visser, J. Low Temp. Phys. **81**, 317 (1990); P. Haen, J. Voiron, F. Lapierre, J. Flouquet, and P. Lejay, Physica B **163**, 519 (1990); G. Bruls, D. Weber, B. Lüthi, J. Flouquet, and P. Lejay, Phys. Rev. B **42**, 4329 (1990).

[26] T. Müller, W. Joss, and L. Taillefer, Phys. Rev. B **40,** 2614 (1989); H. P. van der Meulen, Z. Tarnawski, A. de Visser, J. J. M. Franse, J. A. A. J. Perenboom, D. Althof, and H. van Kempen, Phys. Rev. B **41,** 9352 (1990); J. J. M. Franse, M. van Sprang, A. de Visser, and A. A. Menovsky, Physica B **163,** 511 (1990).

[27] F. R. de Boer, J. J. M. Franse, E. Louis, A. A. Menovsky, J. A. Mydosh, T. T. M. Palstra, U. Rauchschwalbe, W. Shlabitz, F. Steglich, and A. de Visser, Physica B **138,** 1 (1986); A. de Visser, F. R. de Boer, A. A. Menovsky, and J. J. M. Franse, Solid State Commun. **64,** 527 (1987); K. Sugiyama, H. Fuke, K. Kindo, K. Shimohata, A. A. Menovsky, J. A. Mydosh, and M. Date, J. Phys. Soc. Japan **59,** 3331 (1990).

[28] H. Fujii, H. Kawanaka, T. Takabatake, E. Sugiura, K. Sugiyama, and M. Date, J. Magn. and Magn. Mat. **87,** 235 (1990).